Incremental charging method to elucidate the role of (+) trapped charges near the OPC surface in electrostatic image defect formation

Zbig Tokarski and Yong-Jin Ahn, Samsung Electronics, Digital Printing Division, Advanced Development Team, Suwon, Korea; Valentas Gaidelis, Robertas Maldzius, and Tadeusz Lozovski, Dept of Solid State Electronics, Physics Faculty, Vilnius University, Vilnius, Lithuania; and Jonas Sidaravicius, Vilnius Gediminas Technical University, Vilnius, Lithuania

Abstract

An incremental charging method was used to investigate one source of electrostatically induced image defects that produce image ghosting and image spread or blurring. Experimental evidence shows that charge carriers accumulate at the photoconductor surface with each image exposure and that a double charge layer forms at the CTL surface in the exposed (imaged) portion of the OPC drum. These charge carriers are liberated by reversing the surface potential polarity and migrate toward the substrate. The freed positive carriers are neutralized within the charge generation layer by electrons that are injected from the substrate. The incremental charging method attempts experimentally to quantify the charge carrier density in the sub-surface layer and to determine the charge neutralization site upon reverse photoconductor charge.

Introduction

Present-day low-to-high volume electrophotographic printers, copiers, and image reproduction systems require consistent high quality output. One image defect, organic photoconductor (OPC) image ghosting, appears predominately in the half-toned region of a print as a darkened half-tone area of an image that was printed during the previous OPC drum revolution. Another undesirable darker half-tone image phenomenon is line broadening and dot spreading and this appears as a general darkening of the overall image. The occurrence and magnitude of these phenomena depend on OPC layer composition, temperature, humidity, and the number of prints made (electrostatic fatigue) on the OPC drum.

Various ghosting and image spreading models are proposed to account for the image defects produced by an electrically fatigued OPC. Several factors can produce image blurring including lateral motion of i) ions along the photoconductor surface, ii) charges as they vertically transit the charge transport layer (CTL) from the charge generation layer (CGL), and iii) transit carriers that now reside near the surface of the OPC. Image blurring based on an increase in the lateral ion conductivity along the surface and Ohmic conduction with either photoconductor usage [1], an increase in humidity, or special overcoat layers [2] requires time periods that are significantly longer than the time between image exposure to toner development in a real printing system. The time required for charge carriers to transit the charge transport layer is on the order of several milliseconds and far too short for lateral carrier diffusion to produce the magnitude of image and line blurring that is observed experimentally [3,4]. The required lateral travel distance is nearly ¼-½ of the OPC thickness and in a time frame that is about 2 orders of magnitude faster than the exposure-to-development time frame.

The final factor is based on lateral conduction along a very thin surface charge carrier layer at the photoconductor surface. This factor has been modeled, analyzed numerically, and agrees well with the < 0.2 second exposure-to-development printer time scale [5]. This phenomenon increases as the OPC is electrophotographically fatigued and charge carriers build-up during continuous or extended printing.

Electrophotographic fatigue, produced by repeated OPC charging and image exposure, lowers the charging potential voltage and increases residual potential and the dark decay rate. The source is charge carrier trapping in shallow energy wells within the CGL or CTL and the subsequent release of these trapped charge carriers lowers the discharge potential and produces a darker image. The build up of charge carriers trapped in deeper energy wells during extended print cycling increases the residual potential voltage [6] and produces a lighter image. Various other physical phenomena may contribute to these fatigue effects as well.

Some of these electrostatic image defects manifest themselves as charge carrier accumulation at the sub-surface layer and at the two layer boundaries (CGL-CTL or UCL-CGL boundaries) [7]. Charge carrier accumulation and the resulting double electric layer formation is revealed in the incremental charging experiments on various experimental OPC drum samples and the results are presented in this paper.

Experimental

A novel experiment was designed that built up residual trapped charges (holes) near the sub-surface of the OPC and then, by reversing the charging polarity, these charges were forced toward the substrate to recombine with negative charges that migrate through the undercoat barrier layer (UCL). The electrophotographic characterization of several experimental OPC drums prepared with and without an undercoat charge injection barrier layer or using an anodized substrate was used to elucidate the transport of charges across the undercoat and photosensitive layers and to identify the potential source of image defect formation in these different photoconductors.

OPC drums subjected to heat treatment (vs. new drums with no treatment) and repeated exposure to an imaging source (vs. non-imaged drums) were used to collaborate any evidence of the formation of a double charge layer formed at the CTL sub-surface in the exposed (imaged) portion of the OPC drum by monitoring the differences in the charging potentials and dark decay rates.

The dark decay rate and subsequent charging potentials were determined for these samples. Experiments were done by measuring the surface potential for 3 minutes after negative or positive charging and with or without light erasure before the next charging sequence. The charging grid voltage is chosen such that the initial drum potential in the measurement position is equal to (850 ± 20) V. The charging current (ion flux) was kept constant for all photoconductor drums. An alternating charging sequence was employed followed by discharging in the dark (dark decay), i.e., the sequence represented by (–,+,–,+,–,+,–,+,–) indicates an initial negative charging ("–") and a 3 min dark decay period, then positive charging ("+") and a 3 min dark decay period, etc.

OPC samples (Ø24 mm) included a standard reference drum, an experimental dip coated (UCL+CGL+CTL) Drum-1 and ring coated (UCL+CGL+CTL) Drum-2, (polished substrate + CGL + CTL) Drum-3 and (anodized substrate + CGL+ CTL) Drum-4.

Results and Discussion

Incremental Charging

The incremental charging method was used as previously described [7]. Investigating the charge-voltage characteristics of incrementally charged photoconductors provides a lot of information regarding the charge carrier injection-extraction processes that take place in photoconductors. The charge-voltage characteristics of incremental negative and positive charging of a heat treated (50ºC for 162-hour) standard reference photoconductor (Ø24 mm) are shown in Fig.1.

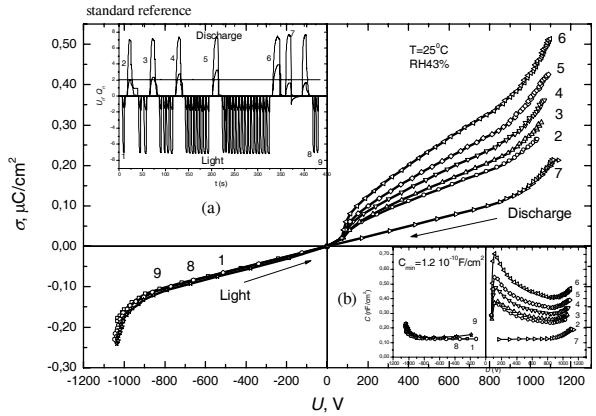

Figure 1. *Charge-voltage characteristics of negative and positive incremental charging of standard reference drum Curve 1 – characteristic of incremental negative charging; 2 – characteristic of incremental positive charging after photoconductor discharge to zero by exposure to red light; 3 – characteristic of incremental positive charging after two cycles of incremental negative charging–discharge to zero by exposure to red light; curves 4, 5 and 6 are the charge-voltage characteristics of positive incremental charging after 4, 8 and 16 cycles of negative charging – discharge to zero by exposure to red light (see inset (a)). Curves 8 and 9 were obtained by repeating the procedures of curve 1; 7 – charge-voltage characteristic of positive incremental charging, obtained after charge-voltage characteristic 6 when the photoconductor is discharged to zero by deposition of negative charge. Inset (b) shows the dependence of effective capacitance on charging potential.*

At first, the photoconductor undergoes incremental negative charging (negative charging deposited in small increments) (curve 1) and then the photoconductor is discharged by exposure to red light. This is immediately followed by incremental positive charging (curve 2). The charge-voltage characteristic of the positive charging becomes nonlinear in the potential voltage range exceeding +100V. The source of the nonlinearity originated during the photodischarge of a negatively charged photoconductor. Holes that were generated by image exposure of the CGL drifted towards the photoconductor surface and a portion of these charge carriers recombined and neutralized the negative ions at the surface. However, a substantial fraction of these holes remain localized in a thin sub-surface region of the photoconductor. These holes are trapped in energy levels of various depths.

During the initial stage of positive incremental charging, the quasi-free holes in the shallowest states begin drifting towards the photoconductor substrate. The deposited charge density incrementally increases but the change in the surface potential voltage is small when the nonlinear region of the charge-voltage curve is reached at ~100-150V. Beyond this region, holes are extracted from progressively deeper states as more positive charges are deposited on the OPC surface and the increase in surface potential voltage is less than that anticipated by geometric capacitive charging alone. The magnitude of the nonlinear region of charge-voltage characteristic will increase as the concentration of holes in the sub-surface states increases. It can be argued that this hole concentration is directly proportional to amount of transitory carriers that did not traverse the surface interface and neutralize the negative surface ions during the initial photodischarge process.

In Fig. 1, the concentration of accumulated holes increases as the number of negative charging + discharge (by exposure to red light) cycles increases prior to positive charging (curves 2 – 6). Subsequent discharge by incremental deposition of negative charge and then positive recharging shows a nearly linear positive charge-voltage characteristic curve for the OPC (curve 7). The next negative charging set (curve 8) also has nearly linear charge-voltage curve and this indicates that no positive charge carriers were available to migrate toward the surface (similar in shape to curves 1 and 9) during the negative charging process.

The nonlinear charge-voltage characteristic observed during incremental charging for the reference photoconductor (Fig. 1, curves 2-6) shows that the sub-surface region of this photoconductor is enriched with hole traps of various energy depths. The linearity of charge-voltage characteristic of negative incremental charging (curve 8) indicates that the substrate barrier – CGL region of the reference photoconductor no longer has any trapped holes. These holes recombined with injected electrons upon reaching the vicinity of the CGL during the positive charging process. This incremental charging pattern is identical for reference photoconductors that were heated prior to charging and those that were not heated.

In contrast, the initial charge-voltage characteristics seen during positive incremental charging of experimental photoconductors (Drums 1-4) are linear up to 100 – 150 V (Fig. 2-5), i.e., only the geometric capacitance (or near to it) of the photoconductor is charged in the initial stage. Subsequently, the increase of potential with deposited incremental charge is very

small (curves 2-6 overlap in this region). This indicates that there are no quasi-free holes in the sub-surface region of the photoconductor and an intense liberation of holes from the sub-surface states begins only after the surface potential reaches 100 – 150 V.

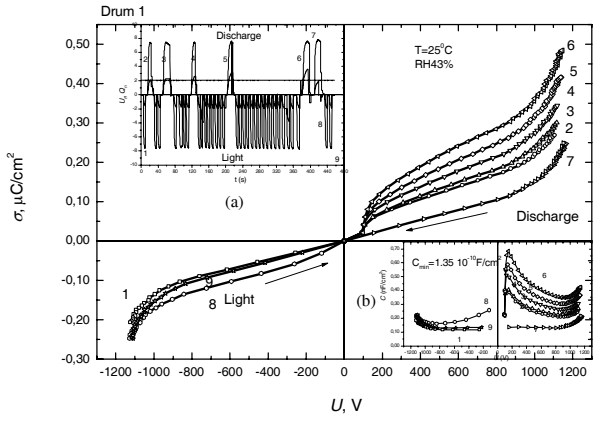

Figure 2. *Charge-voltage characteristics of positive (curves 2–6) and negative (curves 1, 8, 9) incremental charging of experimental Drum-1 (Ø24 mm) after heating at 50ºC for 162-hour. Curve notations are the same as in Fig. 1.*

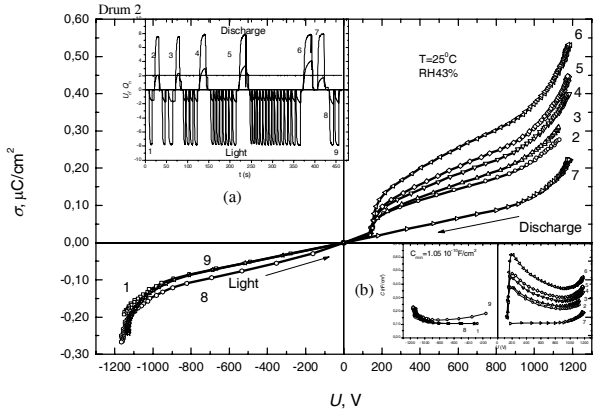

Figure 3. *Charge-voltage characteristics of positive (curves 2–7) and negative (curves 1, 8, 9) incremental charging of experimental Drum-2 (UCL + CGL + CTL, Ø24 mm) drum heat treated for 5 days at 50°C. Curve notations are the same as in Fig. 1.*

These four different experimental photoconductors, in contrast to the standard reference OPC, also display a nonlinear charge-voltage characteristic during negative incremental charging of the drums (Fig. 2-5, curve 8). However, this nonlinearity appears only in situations where the holes that accumulated in the sub-surface region (after negative charging and discharge by light) are forced toward the substrate during a subsequent positive charging. These holes must accumulate near the CGL-UCL interface as the UCL is a hole transport barrier. The nonlinearity in curve 8 during the negative charging stage indicates that the electrons that were injected from the substrate did not neutralize all of the holes. These remaining holes are driven back into the CTL and drift towards the photoconductor surface during the negative incremental charging process.

These experiments show that a very substantial amount of hole accumulation exists within the CGL or at the CGL-UCL / CGL-oxide interface in heat treated Drum-1 (Fig. 2), Drum-2 with UCL (Fig. 3), Drum-3 without UCL (Fig. 4), and Drum-4 with anodized core (Fig. 5). These results are important for explaining the origin of image ghosting. Occasionally, the OPC drum may acquire a positive charge during extensive printing via the positively biased transfer roller that is used to assist image transfer from the OPC drum to paper. This may lead to a lower negative potential in the successive charging cycle and produce an image ghost.

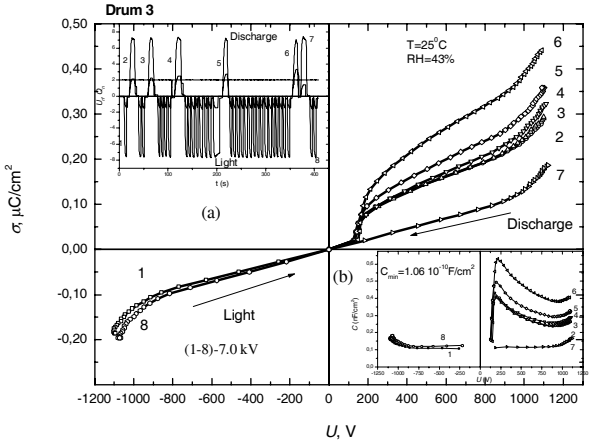

Figure 4. *Charge-voltage characteristics of positive (curves 2–7) and negative (curves 1, 8) incremental charging of experimental Drum-3 (polished + CGL + CTL, Ø24 mm). Curve notations are the same as in Fig. 1.*

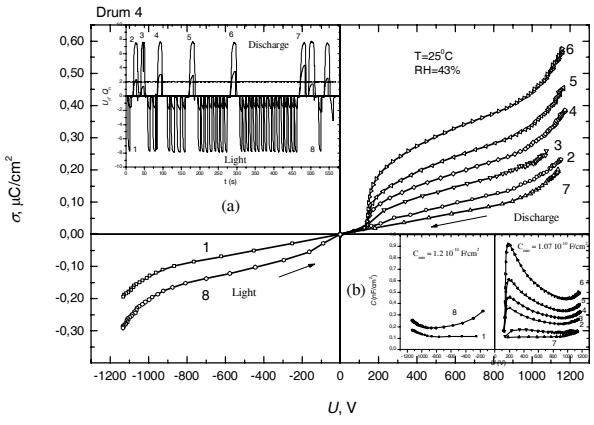

Figure 5. *Charge-voltage characteristics of positive (curves 2–6) and negative (curves 1, 8) incremental charging of experimental Drum-4 (anodized + CGL + CTL, Ø24 mm). Curve notations are the same as in Fig. 1.*

Charging and Dark Decay

This section presents experimental results for charging and dark decay of the reference and experimental drums. The charging potentials of various photoconductors and charge-voltage characteristics during incremental charging were compared before and after thermal treatment, exposure, and adaptation in the dark.

Fig. 6 shows the discharge kinetics for the standard reference drum after heat treatment. The drum was subjected to charging sequence (–, +, –, +, –, +, –) and was exposed to red light with intensity of 40 erg/cm^2 prior to each change in charge polarity.

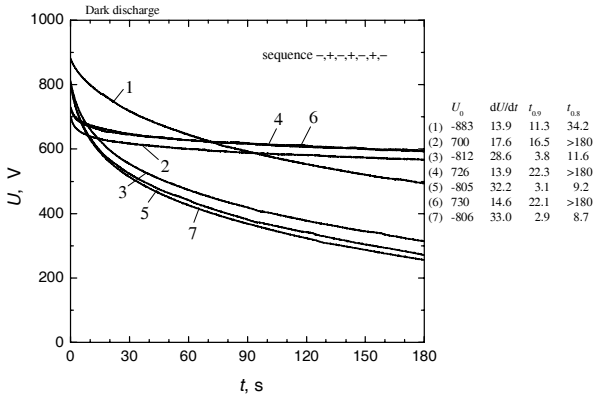

Figure 6. *Discharge of reference (Ø24 mm) drum in the dark. Charging sequence (–, +, –, +, –) taken immediately after the drum was heated at 50°C for 162 hours. Curve 1 – first negative charging; 2 – positive charging after a 3-minute negative discharge; 3 – negative charging after 3-minute positive discharge; similar procedures for curves 4 to 7. Potential decay time to 90% of the initial charge level,·U_0, is $t_{0.9}$ and 80% of·U_0 is $t_{0.8}$.*

Exposure to red light before negative or positive charging decreased in the initial charging potential (without prior exposure (data not shown) $U_{01}^{(-)} = 900$ V and with prior exposure $U_{01}^{(-)} = 858$ V), whereas initial potential dark decay rate noticeably increased (without exposure (dU/dt)i = 13 V/s, and with exposure (dU/dt)i = 20 V/s). The positive potential dark decay rate dU/dt is slow over a wide time range after the initial charging stage, i.e., when the photoconductor is charged after red light illumination (see Fig. 6).

The initial photoconductor potential dark decay rate for the first negative charging is much smaller (especially during the initial 20 s – 30 s) in comparison to the decay rate when the photoconductor was charged negatively after a positive charging (Fig. 6, curve 1 vs. curves 3, 5, 7) for drums with and without prior illumination. This difference between the negative potential dark decay rates is caused by an increase in the hole injection intensity from the CGL into the CTL. Understandably, hole generation intensity in the charge generation layer increases due to an increased electric field across that layer. Discharge of the layer in the dark by applying positive potential after the initial negative charging is achieved due to hole injection from the CGL into the CTL. Electrons in the transport layer are immobile, so hole generation in the bulk can not make the decay rate of negative potential much larger than positive potential decay rate (Fig. 6, curves 1 and 2). When the photoconductor is recharged positively, electrons from the photogeneration layer are driven to the CTL and are trapped at the CTL-CGL interface. When the positively charged photoconductor is negatively recharged, the negative charges that accumulated at the CTL-CGL interface do not disappear (not neutralized), therefore the electric field strength in the CGL increases significantly in comparison with the case of the first negative charging and cause an increase in the dark decay rate, see Fig 7.

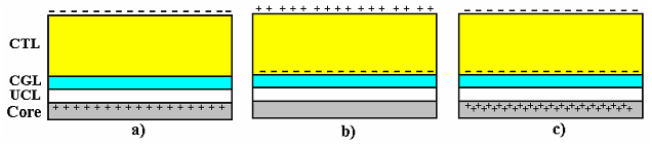

Figure 7. *The diagram of photoreceptor charging-recharge: a) after the first negative charging; b) after the following positive charging; and c) after the third negative charging.*

The time dependences for the dark decay potential to decrease for Drum-1 photoconductor (Fig. 8), charged in the sequence (–, +, –, +, –, +, –, +, –), are quite different from the corresponding dependences for the reference photoconductor (Fig. 6). In contrast to reference photoconductor, whose negative and positive potential dark decay rates are strongly different, Drum-1 photoconductors are characterized by small differences between the negative and positive potential dark decay rates (Fig. 8). In addition, the discharge kinetics for Drum-1 photoconductor after the first charging are almost identical to the discharge kinetics after subsequent charging cycles (Fig. 8, curves 1, 3, 5, 7, 9).

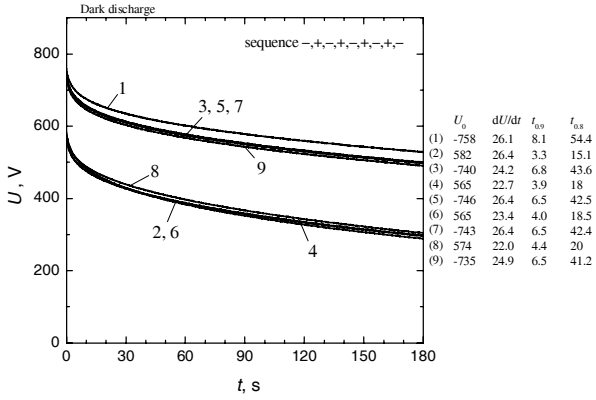

Figure 8. *Dark decay of negative (curves 1, 3, 5, 7, 9) and positive (2, 4, 6, 8) potentials for Drum-1 (Ø24 mm) drum. Charging was done after erasure by light and 6 weeks after heating at 50°C for 162 hours. Notations of curves are the same as in Fig. 6.*

When charging was done after illumination, the initial negative potential of Drum-1 photoconductors decreased and the initial potential dark decay rate increased from (dU/dt)i = 7.3 V/s (without action of light) up to (dU/dt)i = 26 V/s (with action of light). Similar regularities were observed for the positive potential time dependences.

Based on comparisons between the initial charging potential levels, initial potential dark decay rates, and the potential kinetics over a wide range of times, the Drum-2, Drum-3, and Drum-4 photoconductors are more similar to Drum-1 photoconductor in

electrostatic behavior than to the reference photoconductor (Fig. 9-11). Potential kinetics of Drum-2 (UCL + CGL + CTL) photoconductors during charging and discharge in the dark is strongly influenced by the illumination of light before charging. The initial negative charging potential without and with prior illumination was $U_{01}^{(-)} = 938$ V and $U_{01}^{(-)} = 876$ V, respectively (Fig. 9). The negative charging potentials stay almost the same in charging cycles from 2 to 4 (Fig. 9, curves 3, 5, 7).

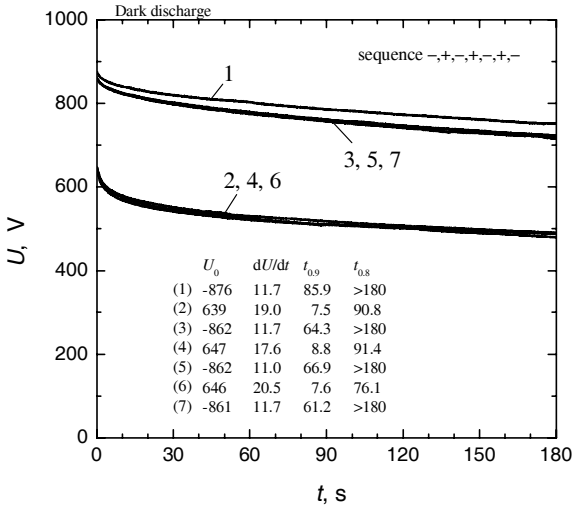

Figure 9. *Discharge of negative and positive potential in the dark of Drum-2 (UCL + CGL + CTL, Ø24 mm) after negative charging (curves 1, 3, 5, 7) and positive charging (2, 4, 6); with erasure by light; no prior heating. Charging sequence is the same as in Fig. 6.*

The initial potential dark decay rate is 2–3 times higher in all cases with prior illumination than without illumination. The negative potential dark decay rate of a photoconductor formed on a polished substrate (Fig. 10) is faster than negative potential decrease of a photoconductor formed on an anodized substrate (Fig. 11).

Table 1 lists the differences of the dark decay rates without and with prior illumination, which is significant for ghosting to appear. The biggest difference between dark decay rates for the non-illuminated and illuminated cases is for Drum-1. Ghosting was present in Drum-1 drum and this is in accordance with the model described above. This produces different potentials on the image elements in the places that where exposed or not exposed in the previous cycle and to ghost appearance as previously discussed.

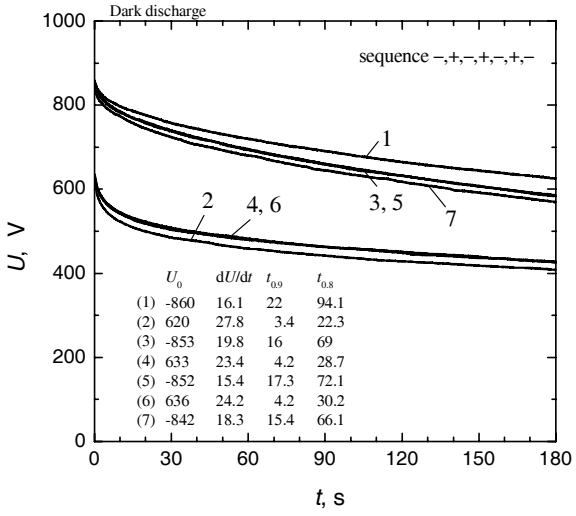

Figure 10. *Discharge of negative and positive potential in the dark of Drum-3 (polished + CGL + CTL, Ø24 mm) after negative charging (curves 1, 3, 5, 7) and positive charging (2, 4, 6); with erasure by light and no prior heating. Charging sequence is the same as in Fig. 6.*

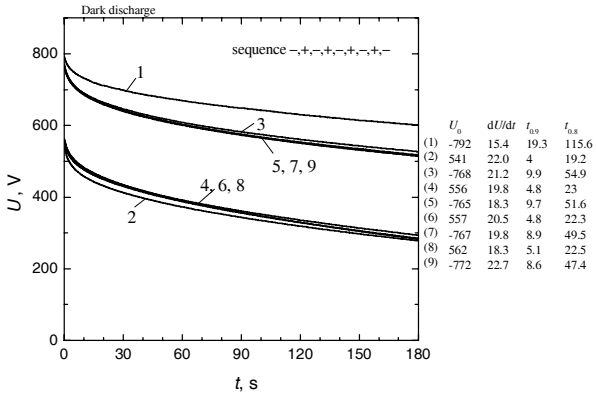

Figure 11. *Discharge of negative and positive potential in the dark of Drum-4 (anodized + CGL + CTL, Ø24 mm) after negative charging (curves 1, 3, 5, 7, 9) and positive charging (2, 4, 6, 8); with erasure by light and no prior heating. Charging sequence is the same as in Fig. 6.*

In addition, the differences in the charging potentials and dark decay rates of OPC drums suggested that a double charge layer formed at the CTL surface in the exposed (imaged) portion of the OPC drum. Upon reversing the charging polarity, holes from the surface double layer traveled through the CTL and either fully recombined with electrons at the CGL-UCL interface or partially

Table 1. Initial Dark Decay Rates for Curve 1

Drum ID	$(dU/dt)_i$ (V/s)	
	After dark	After prior illumination
Reference	13.2-16.1	13.9-20.5
Drum-1	5.9-7.3	22.7-26.1
Drum-2	1.5	11.7
Drum-3	5.9	16.1
Drum-4	4.4	15.4

accumulated at that interface in drums that displayed image defects but was practically absent in defect-free drums. These accumulated holes influence negative charging in subsequent charging of the OPC drum and lead to a lower surface potential and darker ghosting image on a half-tone gray background image.

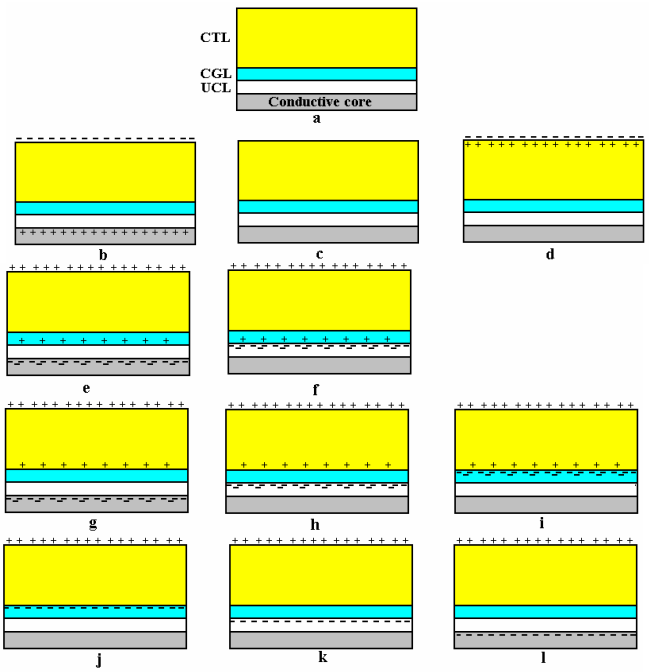

Figure. 12. *Charge distributions in the OPC according to the incremental charging results.*

Fig. 12 illustrates the charge distributions schemes drawn on the basis of these investigations. The situations are described as follows: (a) not charged OPC, (b) negatively charged OPC, (c) OPC discharged by deposition of charges of opposite polarity, (d) negatively charged and discharged by illumination OPC, a double electric layer is formed at the sub-surface region. The cases (e) through (l) represent possible charge distributions after positive charging of the OPC with double electric layer in the sub-surface region (case (d)).

Experimental Drum-1 can be described by either case (e) or case (f). The low hole accumulation during positive charging excludes cases (g) to (i) for Experimental Drum-3 (without the UCL). The reference drum should be represented by case (j). Cases (k) and (l) are not supported by the results of dark discharge investigations (negative potential dark discharge speeds up after positive charging).

Conclusion

Characterization of the OPC samples by incrementally charging the photoconductor (small ΔV increments) indicated that charges (holes) accumulated at sub-surface region of CTL in cycles with negative charging and image exposure in all the drum samples and these charges were driven towards the core during the positive charging stage (as may occur during transfer of toner from OPC to paper).

These holes can then either fully recombine with electrons at the CGL-UCL interface or partially accumulate at the interface. It was determined that holes accumulated at the UCL-CGL interface in the experimental Drums (1 to 4) but not in the reference drum. These accumulated UCL holes influence negative charging and may lead to lower surface potentials and ghosting.

The effective capacitance values, measured upon positive re-charging, were too large to account for negative charge induced ghosting that would be produced by negative charge migration over a short distance and then trapping within the barrier and charge generation layers.

Differences in charging and dark decay behavior, in view of the ghosting causes, seems to be related to the different sensitivities of the drums to prior illumination (image exposure); and the differences in the charging potentials and dark decay rates measured with exposure or without prior illumination. This may lead to a bigger difference in surface potentials in these two regions and appear as a darker ghost image on a gray background.

References

[1] E. J. Yarmchuk and G. E. Keefe, "Motion of surface charge on layered organic photoconductor," J. Imaging Sci. 35, 232 (1991)

[2] D.S. Weiss, J.R. Cowdery, W.T. Ferrar, and R. H. Young, "Analysis of Electrostatic Latent Image Blurring Caused by Photoconductor Surface Treatments," J. Imaging Sci, 40, 322 (1996)

[3] J. Yi and R. B. Wells, PC surface charge density from a vertically Gaussian, laterally exposure-based volume charge distribution in the CGL, *Proc. IS&T's NIP 19 International Conference on Digital Printing Technologies,* IS&T Springfield VA, 2003, pp. 91-96

[4] Y. Watanabe, H. Kawamoto, H. Shoji, H. Suzuki, and Y. Kishi, "A Numerical Study of High resolution Latent Image Formationby Laser Beam Exposure," J. Imaging Sci. 45, 579-586 (2001)

[5] J. Yi and R. B. Wells, "Numerical simulation of the lateral conductivity of a photoconductor surface," J. Imaging Sci. 48, 294 (2004)

[6] C-W Lin, T Nozaki, and Y. Hoshino, Analysis of Traps in Photosensitive Materials from the Dependence of Corona Charging Characteristics on Exposure, *Proc. IS&T's NIP 13 International Conference on Digital Printing Technologies,* IS&T Springfield VA, 1997, pp. 270-273

[7] E. Montrimas, T. Lozovski, J. Sidaravicius, Z. Tokarski, "Charging Transients of Organic Electrophotographic Photoconductors," J. Imag. Sci., 49, 326 (2005)

Author Biography

Zbig Tokarski received his Ph. D. in Engineering from the University of Connecticut, Storrs CT, USA. Over the past 15 years, he has developed organic opto-electronic and electrophotographic materials for advanced applications. Dr. Tokarski has worked for Samsung Electronics since 2000 in the US and Korea and is currently a principal engineer in the Digital Printer Division, Advanced Development Team in Suwon, Korea.